JOURNAL OF
THE ENGINEERING
MECHANICS DIVISION

PORE PRESSURE AND DRYING OF CONCRETE AT HIGH TEMPERATURE

By Zdeněk P. Bažant,[1] M. ASCE and Werapol Thonguthai[2]

INTRODUCTION

The magnitude of pore pressures and the loss of moisture caused by heating of concrete is of considerable concern for predicting the response of prestressed concrete nuclear reactor vessels to hypothetical core disruptive accidents as well as the response of concrete structures to fire. There exists a vast amount of literature (8,12,14,18,22,26–29,33,35,38) concerned with directly measurable properties of concrete at high temperatures and empirical practical prediction of fire resistance. Recently, more sophisticated predictions of fire resistance and, in particular, of shrinkage and stresses induced by drying in fire exposure have been studied by Bresler, et al. (8,11–13), and others (2,23,24,26,38). As far as comprehensive and rationally based mathematical models for the behavior of concrete are concerned, only the temperature range up to 100° C has been explored to any significant extent. It appears that no physical mathematical model for concrete exposed to temperatures above 100° C has been attempted so far. This is the objective of this paper.

FIELD EQUATIONS OF COUPLED HEAT AND MOISTURE TRANSFER IN CONCRETE

We face a problem of coupled heat and mass transfer in a porous solid undergoing microstructural and chemical changes. Although the general approach within the framework of irreversible thermodynamics is well known, the problem in its full detail is extremely complex and must, therefore, be simplified.

One important characteristic of heat and moisture transfer in porous solids is their coupling. Thus, the flux of moisture in concrete, $\underset{\sim}{J}$, in kg/m^3 s, should consist of the flux due to the gradient of moisture concentration w (Fick's

Note.—Discussion open until March 1, 1979. To extend the closing date one month, a written request must be filed with the Editor of Technical Publications, ASCE. This paper is part of the copyrighted Journal of the Engineering Mechanics Division, Proceedings of the American Society of Civil Engineers, Vol. 104, No. EM5, October, 1978. Manuscript was submitted for review for possible publication on October 14, 1977.

[1]Prof. of Civ. Engrg., Northwestern Univ., Evanston, Ill.
[2]Grad. Research Asst., Northwestern Univ., Evanston, Ill.

law of diffusion), as well as the flux due to the gradient of temperature T (Soret flux). Similarly, the heat flux, q, should consist of a flux due to the gradient of temperature T (governed by the Fourier law), and the flux due to the gradient of moisture concentration (Dufour flux). Accordingly

$$\underset{\sim}{J} = -a_{ww}\,\text{grad}\,w - a_{wT}\,\text{grad}\,T \quad (1a)$$

$$\underset{\sim}{q} = -a_{Tw}\,\text{grad}\,w - a_{TT}\,\text{grad}\,T \quad (1b)$$

in which w = mass of all free (not chemically bound) water per m^3 of concrete; this represents all water that is evaporable at a given temperature. Coefficients a_{ww}, a_{wT}, a_{Tw}, and a_{TT} depend on w and T. Note that, generally, $a_{wT} \neq a_{Tw}$ because grad w and grad T are not the thermodynamic forces associated with fluxes J and q (21,32,43).

Eqs. 1*a* and 1*b* are written under the assumption that fluxes J and q are independent of the strains in concrete. This must be almost exactly true for several reasons: (a) The volumetric compressibility of water phase in concrete is much higher than the volumetric compressibility of concrete (even when the pores are completely saturated by liquid water); (b) the changes of pore space that can be produced by deformations of concrete are much less than the total relative volume change of concrete; and (c) the heat produced by the work of stresses in concrete is negligible.

Because w is a function of temperature T and pore water pressure p, $w = w(p, T)$, Eq. 1*a* may be rearranged as

$$\underset{\sim}{J} = -\frac{a}{g}\,\text{grad}\,p - a_1\,\text{grad}\,T \quad (2)$$

in which g = 9.806 m/s^2 = gravity acceleration (included for reasons of dimensionality); and $a/g = a_{ww}(\partial w/\partial p)_T$, $a_1 = a_{wT} + a_{ww}(\partial w/\partial T)_p$. Eq. 2 has the advantage that the thermal gradient contribution, a_1 grad T, appears to be rather small, as studies of test data indicated. So, approximately, $a_1 \approx 0$; i.e., we may assume a single potential to govern the moisture transfer and we have:

$$\underset{\sim}{J} = -\frac{a}{g}\,\text{grad}\,p \quad (3)$$

in which a = permeability, in m/s. Eq. 3 is, of course, the same as Darcy's law. However, this law is, in principle, limited to saturated porous media. It is one major finding of this paper that the Darcy-type law applies for both saturated and nonsaturated concrete, provided that pressure in the pores of nonsaturated concrete is interpreted as the pressure of water vapor rather than the pressure of capillary water. This finding is a result of extensive data fitting described in the sequel, in which nonzero a_1 has been considered and best fits were obtained when a_1 was roughly zero.

Thus, compared to w as well as other possible variables that might be chosen for the driving force governing moisture transfer, pore pressure p appears to be more convenient because it allows eliminating the effect of grad T upon J [as has been intuitively suggested before (5)]. Despite that, however, Eq. 3 also gives a certain thermal moisture flux (Soret flux, Eq. 1*a*); indeed, substituting grad p = $(\partial p/\partial w)$ grad w + $(\partial p/\partial T)$ grad T, we see that Eq. 3 is a special case of Eq. 1*a* with $a_{ww} = ag(\partial p/\partial w)_T$ and $a_{wT} = ag(\partial p/\partial T)_w$. For nonsaturated concrete at uniform temperature, Eq. 2 is equivalent to the previously used relation $J = \bar{a}$ grad h (7,9) in which $h = p/p_s(T)$, $p_s(T)$ being the saturation vapor pressure.

The coupled heat flux in Eq. 1*b* may be also neglected, as data fits in the sequel confirm, and, setting $a_{TT} = b$ = heat conductivity, we may write

$$\underset{\sim}{q} = -b\,\text{grad}\,T \quad (4)$$

The condition of conservation of the mass of water normally reads $\partial w/\partial t = -\text{div}\,J$. However, at room temperature this equation requires correction for the water consumed by hydration, and a further (larger) correction is required to account for the water released by dehydration due to heating, the reverse of hydration. Since w is defined to include all free (i.e., evaporable, not chemically combined) water (19,20,35,39), conservation of mass requires that

$$\frac{\partial w}{\partial t} = -\text{div}\,\underset{\sim}{J} + \frac{\partial w_d}{\partial t} \quad (5)$$

in which w_d = total mass of free (evaporable) water that has been released into the pores by dehydration. At temperatures above 120° C, w_d increases. For $T \leq$ 100° C, we may set $\partial w_d/\partial t = -\partial(\Delta w_h)/\partial t$ and use the same term to account for the water deficiency, Δw_h, that is created in the pores by hydration (6) and is manifested by self-desiccation (7,9,19); $\Delta w_h/\rho_w$ equals the combined volume of anhydrous cement grains and water from which the cement gel formed, minus the volume of the cement gel produced. This difference is much less than the amount w_h of water consumed by hydration (ρ_w = mass density of liquid water, 1 g/cm^3).

The balance of heat requires that

$$\rho C\frac{\partial T}{\partial t} - C_a\frac{\partial w}{\partial t} - C_w \underset{\sim}{J}\cdot\text{grad}\,T = -\text{div}\,\underset{\sim}{q} \quad (6)$$

in which ρ, C = mass density and isobaric heat capacity of concrete (per kilogram of concrete) including its chemically combined water, but excluding its free water; C_a = heat of sorption of free water (per kilogram of free water); C_w = mass density and isobaric heat capacity of bulk (liquid) water; and $C_w J \cdot$ grad T = rate of heat supply due to heat convection by moving water. This term may be derived by expressing the increase in heat content as $-wC_w\Delta T$, in which $\Delta T = \Delta x(\partial T/\partial x)$ = temperature difference over distance $\Delta x = v_x \Delta t$ and $v_x = J_x/w$ = mean velocity of water. Usually, the heat convection term is negligible, but in rapid heating it might not be so.

Equation of State of Pore Water

While the general form of the field equations is clear, considerable uncertainty stems from the material properties. Following the general approach suggested before (5), we will present here an approximate, but rational, constitutive relation for pore pressure p, water content w and temperature T, assuming that a local thermodynamic equilibrium always exists between all phases of pore water within a small element of concrete. No doubt this assumption is practically exact.

Nonsaturated Concrete.—For temperatures below the critical point of water (374.15° C), we must distinguish between saturated and nonsaturated (partially saturated) concrete. Consider first nonsaturated concrete, $p \leq p_s(T)$. Due to scarcity of test data, it is worth trying to obtain some theoretical information. We will now derive a simple temperature dependence of the p-w relation, assuming the pore geometry to be invariable, and the amount of adsorbed water to be negligible. The pressure in capillary (liquid) water may be expressed as $p_c = RM^{-1}\rho_w \hat{T} \ln h = 2\gamma(T)/r$ in which $h = p/p_s$; ρ_w = mass density of liquid water (1 g/cm^3); $\hat{T}$ = absolute temperature; r = radius of capillary menisci; and γ = surface tension of water. Consider now that temperature is changed while keeping the amount of pore water, w, constant. Then (if the effect of

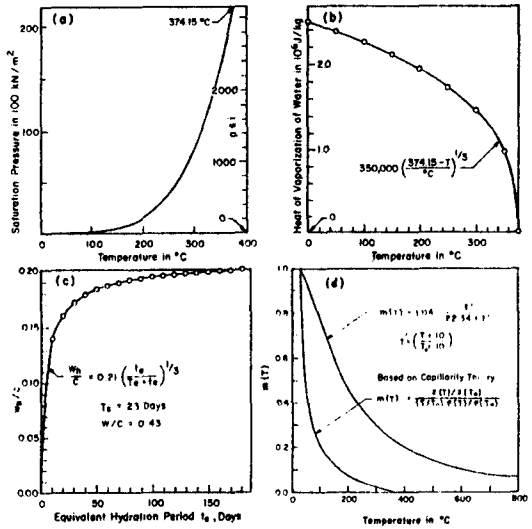

FIG. 1.—(*a*) Saturation Pressure of Water Based on ASME Steam Tables (3); (*b*) Fit of ASME Steam Table Values on Heat of Vaporization of Water; (*c*) Fit of Powers and Brownyard's Data (39) on Hydration Water; (*d*) Exponent $m(T)$ for Temperature Dependence of Sorption Isotherms

nonuniqueness of capillary surface for given r is neglected), r must also remain roughly constant, and expressing $1/r$ from the preceding relation, we conclude that $(\rho_w \hat{T}\gamma)\ln h$ = constant (5). Denoting $m = (\rho_{w_0}\hat{T}_0/\gamma_0)/(\rho_w \hat{T}/\gamma)$ in which subscript 0 denotes the values at reference temperature 25° C, we further see that $(\ln h)/m$ = constant or $h^{1/m}$ = constant if w is constant (5). According to experimental data (25,36,39,42) for dense cement pastes at 25° C, $w/w_s \approx h$ in which w_s = water content at pore saturation. Combining this with $h^{1/m}$ = constant, we conclude that $w/w_s = h^{1/m} = [p/p_s(T)]^{1/m}$ at variable temperature [Fig. 1(*d*)]. Here, function $p_s(T)$ is known exactly (3) [Fig. 1(*a*)], while exponent m has been related above to the temperature dependence of surface tension, $\gamma = \gamma(T) = B[(\hat{T}_c - \hat{T})/\hat{T}_c]^{\mu}[1 + b(\hat{T}_c - \hat{T})/\hat{T}_c]$; $\hat{T}_c$ = 647.15° K, B = 258,000 N/m, $b = -0.625$, and $\mu = 1.256$ (34).

However, when the aforementioned expressions for m and w/w_s were used, satisfactory fits of test data could not be achieved, although the response was qualitatively reasonable. The pressures, p, were much too high, and this also caused water to leave a heated specimen much too fast. Moreover, for the critical point of water, the last equation gives $m = 0$, which would incorrectly imply that no evaporable water could be held above 374.15° C. In view of the simplifying assumptions made, these discrepancies are not surprising. In fact, a different temperature dependence could be theoretically derived if all pore water were assumed to consist of the (unhindered) adsorbed water that follows the BET isotherm (15).

It thus becomes apparent that the preceding theoretical derivation can be used only for rough guidance, in that a power function of h with a temperature-dependent exponent, m, is appropriate. Function $m(T)$, however, must be empirically corrected. By the fitting of test data (23,46,47), it has been found that the following semi-empirical expression [Fig. 1(*d*)] is acceptable:

$$\frac{w}{c} = \left(\frac{w_1}{c}h\right)^{1/m(T)} \quad \text{with} \quad h = \frac{p}{p_s(T)}, \quad \text{for} \quad h \leq 0.96 \quad \ldots\ldots\ldots\ldots (7)$$

$$\text{in which} \quad m(T) = 1.04 - \frac{T'}{22.34 + T'}; \quad T' = \left(\frac{T + 10}{T_0 + 10}\right)^2 \quad \ldots\ldots\ldots (8)$$

Here, T = temperature, in °C; T_0 = 25° C; c = mass of (anhydrous) cement per m^3 of concrete; and w_1 = saturation water content at 25° C (3) (see Fig. 5 in the sequel; the limit of 0.96 is explained later). Note that according to Eq. 7, the saturation water content is $w_s = c(w_1/c)^{1/m(T)}$, i.e., at a higher temperature the saturated state is reached at a lower water content. It has been also tried to use $w = w_1 h^{1/m}$ which gives a temperature-independent water content at saturation; this, however, did not allow satisfactory fits. It is also convenient that w_1/c can be accurately determined for a given concrete mix (35,39).

Saturated Concrete.—It may seem, at first, that pore pressure p in saturated concrete could be calculated directly from w and T using thermodynamic steam tables (3) and taking the porosity, n, as the given volume available to pore water. However, for concrete that is perfectly saturated at 25° C and then heated beyond 100° C, this would yield enormous pore pressures. For example, if porosity increased by 2%, pore pressure would build up to 1,000 atm at 130° C and over 10,000 atm at 300° C. If there is no change in porosity, then the pore pressure at 100° C would be around 1,000 atm, even if the pore space is considered to increase due to the elastic volume expansion produced by pore pressure. So, we could get nowhere close to reasonable pore pressure values.

The only possible explanation is that the pore space available to capillary water, which constitutes about 70%–80% of w and represents that part of water to which the thermodynamic steam tables (3) must apply (they cannot be applied to adsorbed water), greatly increases with temperature as well as pressure. This conclusion is one major result of this paper. The increase is partly due to an increase of the total pore space, but more significantly it is due to a decrease of the adsorbed water portion in total water w. Taking a closer look at the microstructure, we see that such an explanation is entirely reasonable,

indeed necessary. For instance, from studies of sorption isotherms at room temperature (25,39,44) it is well known that the internal surface area greatly varies on drying and rewetting, and so the same must be expected at $p > p_s$ and at higher temperatures.

The thermodynamic properties of water (3) may be introduced in terms of the specific volume, v, of water as a function of T and p, $v = v(T,p)$. Then the effect of porosity change and of elastic volume expansion may be described by

$$w = (1 + 3\epsilon^v)\frac{n}{v} \quad \text{for} \quad h = \frac{p}{p_s} \geq 1.04 \quad \ldots\ldots\ldots\ldots\ldots\ldots\ldots (9)$$

in which $d\epsilon^v = d\sigma^v/(3K) + \alpha dT$; and $\sigma^v = np$. Here, n = porosity; ϵ^v = linear volumetric strain of concrete due to the resultant, σ^v, of pore pressure; K = bulk modulus; and α = coefficient of linear thermal dilatation of concrete, typically, $5 \times 10^{-6}/°\,C$–$12 \times 10^{6}/°\,C$ (35). (The limit of 1.04 is clarified later.)

From measurements, it is known that porosity increases with temperature (26,28). This is explained by partial dehydration, i.e., the release of some water molecules that were chemically bound at room temperature. The amount, w_d, of water that is released by dehydration is also known (20,27,28). Taking the average mass density of chemically bound water to be the same as for liquid water at 25° C, $\rho_0 = 1{,}000\ kg/m^3$, we would have $n = n_0 + (w_d - w_{d_0})/\rho_0$ in which $w_d - w_{d_0}$ = decrease of weight (per m^3) of chemically bound water from $T_0 = 25°$ C to T; and $n_0 = n$ at room temperature. However, the average mass density of combined water molecules before dehydration is impossible to determine, and aside from that it is also necessary to consider the aforementioned increase of the pore space available to water as pressure increases. Therefore, we may introduce an empirical correction function, P, as follows:

$$n = \left[n_0 + \frac{w_d(T) - w_{d_0}}{\rho_0} \right] P(h) \quad \text{for} \quad h \geq 1.04 \quad \ldots\ldots\ldots\ldots\ldots (10)$$

$$\text{with} \quad P(h) = 1 + 0.12(h - 1.04), \quad h = \frac{p}{p_s(T)} \quad \ldots\ldots\ldots\ldots\ldots (11)$$

Function P has been identified by fitting test data, while $w_d(T)$ has been taken according to measurements of weight loss of specimens of heated concrete in thermodynamic equilibrium (26–28). This function has been defined in a computer program by a set of values according to measurements of Harmathy (27,28).

As already mentioned, the increase of pore space due to pore pressure is mainly a manifestation of a reduced proportion of adsorbed water, to which thermodynamic steam tables (3) do not apply; but, partly, it is also due to the actual increase of the total pore space. From this point of view, it might have been more logical to write Eq. 9 in terms of the capillary porosity, n_{cap}, rather than total porosity n for all evaporable water including the adsorbed water. However, calculation of n_{cap} would complicate the formulation.

Saturation Transition.—Due to a wide range of distribution of pore sizes, and to very slow water exchange between large and small pores, it is likely that pressures in excess of $p_s(T)$ may develop in the smallest pores before

$p_s(T)$ is reached in adjacent large pores. Thus, the transition from saturated to unsaturated state would not be abrupt, except perhaps for an extremely slow change in pore pressure p giving enough time for the pressures to equilibrate among all pores. In addition, an abrupt transition would cause computational difficulties, impairing the convergence of iterations in individual time steps. Moreover, it should be realized that measurement of pore pressures near saturation is rather unreliable and poorly reproducible (39). For all these reasons, it is

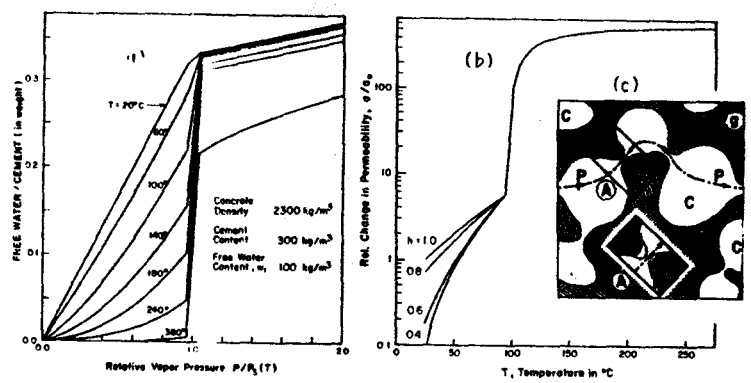

FIG. 2.—(a) Sorption Isotherms; (b) Dependence of Permeability on Temperature and Humidity; (c) Flow Passage in Cement Gel, with Neck

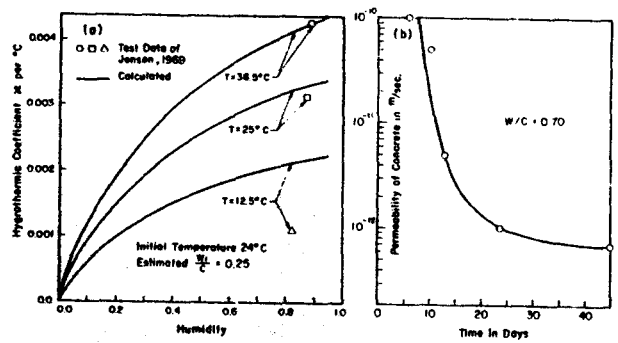

FIG. 3.—(a) Fit of Jensen's Measurements (31) of Hygrothermic Coefficient; (b) Fit of Powers and Brownyard's Data (39) on Permeability Dependence on Age

logical to introduce an empirical transition region. The transition is considered as a straight line joining the value $w = w_{96}$ from Eq. 7 for $h = p/p_s(T) = 0.96$ and the value $w = w_{104}$ from Eq. 9 for $h = 1.04$, both for the same T.

The set of sorption isotherms as given for various temperatures by Eqs. 7–12 is plotted in Fig. 2 for a particular concrete. A partial check is provided by a comparison [Fig. 3(*a*)] with Jensen's measurements (31) of hygrothermic coefficient $\kappa = \partial h/\partial T$ for a sealed specimen (constant total water content $w + w_d$).

When comparing the permeability of cement paste and concretes at room temperature, Powers (39) found that the major variable is the capillary porosity, n_c, of cement paste, which itself depends mainly on the water-cement ratio and the degree of hydration (or age) [see Fig. 3(*b*)]. However, from a theoretical point of view, neither the capillary porosity, n_c, nor the total porosity, n, can be the basic factor, because moisture transfer below 100° C is not controlled by the flow of capillary (liquid) water. For explanation, it may be assumed that the capillary pores are not continuous (20) and that the flow is controlled by the minimum pore cross sections or "necks" on the continuous flow passages through the cement paste (*P* in Fig. 2*c*). (Among all parallel passages, it is those with the largest neck widths that matter.) In dense cement pastes, the necks are perhaps only about 50 Å wide, which means that the neck can contain only adsorbed water, but no liquid water or vapor. Even if the neck is not completely filled by water, hardly any vapor can pass because the mean free path of vapor molecules (about 800 Å at 25° C and 1 atm) greatly exceeds the neck size.

From these facts, it has been inferred by Powers and others that at low temperature the mechanism of moisture transfer is controlled by the migration of molecules along the adsorbed water layers. At first, this might seem to cast doubt on our assumption that moisture transfer in nonsaturated concrete is governed by the pressure of water vapor in the pores. However, our assumption is consistent. To show it, γ may be calculated from the relation $d\gamma = -RM^{-1}\hat{T}\,\Gamma_a dp/p$ (4,7), in which R = gas constant; M = molecular weight of water; $\hat{T}$ = absolute temperature; Γ_a = surface mass concentration of adsorbed water (g/cm^2). Approximately, $\Gamma_a \approx \Gamma_1 p/p_s(T)$ in which Γ_1 = constant. Then, integration of $d\gamma$ yields $\gamma = \gamma_s(T) + RM^{-1}\Gamma_1\hat{T}(1-h)$ in which $h = p/p_s(T)$ and γ_s is the surface tension at saturation. The variation of γ_s with T has little effect, and so γ varies almost linearly with p, as well as h. So, taking grad p or grad h as the driving force of adsorbed water diffusion is roughly equivalent.

For temperatures exceeding 100° C, it has been found from the test data presented here that permeability increases by about two orders of magnitude.

One could try to explain it simply by a drastic increase in mobility of adsorbed water (as suggested to the writers by F. H. Wittmann of Delft), but a physical mechanism of this is unclear. Explanations by an overall porosity increase, by the decrease in the mean free path of water molecules, or by the thinning of adsorbed water layers in the necks are insufficient to explain a permeability increase by two orders of magnitude. We will propose here a more plausible hypothesis: Due to smoothing of pore surfaces to reduce the surface energy, the width of the necks governing the flow (*N* in Fig. 2*c*) increases many times as T exceeds 100° C, allowing water to pass through the necks in vapor or liquid state while at the same time the pore volume of the necks is negligible, so that no significant effect of a large relative increase of neck width upon the measured pore size distributions at high T can be detected. Thus, whereas at room temperature the neck width must be related to n_c (or else Powers' dependence of permeability upon n_c could not be true), at high T this relationship would break down.

The fact that the necks should be of subcapillary size is also suggested by the finding (9) that at room temperature the permeability decreases about 20 times as h is lowered from 0.9 to 0.6. Indeed, the only reasonable explanation seems to be that the mechanism of moisture transport in the necks is migration of water molecules within the adsorbed water layers, which get thinner as the relative humidity is lowered and hold, therefore, the migrating water molecules more strongly. In view of this mechanism, it was previously proposed (9) that below 100° C the dependence of permeability upon temperature is not governed by viscosity of liquid water or vapor, but by the activation energy, Q, for the migration of absorbed water molecules along the walls of necks.

In consequence of this picture, permeability a, which figures in Eq. 2, may be introduced in the form

$$\text{For } T \le 95^\circ\text{ C}: \quad a = a_0 f_1(h) f_2(T) \qquad (12a)$$

$$\text{For } T > 95^\circ\text{ C}: \quad a = a_0' f_3(T) \quad \text{with} \quad a_0' = a_0 f_2(95^\circ\text{ C}) \qquad (12b)$$

in which a_0 is the reference permeability at 25° C. Temperature 95° C is chosen to represent the beginning of the transition. Function $f_1(h)$ reflects the moisture transfer within the adsorbed water layers in the necks, and, according to Refs. 7 and 9

$$f_1(h) = \alpha + \frac{1-\alpha}{1+\left(\dfrac{1-h}{1-h_c}\right)^4}, \quad \text{for } h \le 1;\ f_1(h) = 1, \quad \text{for } h \ge 1 \qquad (13)$$

in which $h_c \approx 0.75$ = transition humidity and $\alpha \approx 1/20$ at 25° C. For 95° C, we assume the necks to be wide enough for the water to be transfered as liquid or vapor. Thus, α must equal 1.0 at 95° C. For α values between 25° C and 95° C, a linear interpolation has been used in all data fits shown. However, subsequently it appeared that $1/\alpha = 1 + 19(95 - T)/70$ might have been more appropriate with regard to extension below 25° C.

The temperature dependence of permeability below 95° C is given by Arrhenius-type equation

$$f_2(T) = \exp\left[\frac{Q}{R}\left(\frac{1}{\hat{T}_0} - \frac{1}{\hat{T}}\right)\right]; \quad T \le 95^\circ\text{ C} \qquad (14)$$

in which $\hat{T}$ = absolute temperature; Q = activation energy for water migration along the (multimolecular) adsorption layers in the necks; and R = gas constant. According to Ref. 9, $Q/R \approx 2{,}700^\circ$ K.

Function $f_3(T)$ has been found to yield, between 95° C and 105° C, a jump by two orders of magnitude. The jump is imagined to correspond to the transition from the moisture transfer mechanism governed by the activation energy of adsorption to a mechanism governed by viscosity of a mixture of liquid water and steam. After the transition is completed (around 105° C), function $f_3(T)$ should follow the temperature dependence of viscosities of water and steam; above 105° C, both of them vary relatively little, and so $f_3(T)$ beyond 105° C should be almost constant. All these properties may be described by

$$f_3(T) = \exp\left[\frac{T-95}{0.881+0.214(T-95)}\right];\quad T>95^\circ\text{C} \qquad (15)$$

in which T is in °C; and the numerical constants have been determined by fitting the test data.

Aside from temperature and pore pressure effects, permeability is also drastically influenced by the degree of hydration (or age). According to available test data, it seems that this may be well described as

$$a_0 = a_1 10^{\sqrt{a_2/t_e}} \qquad (16)$$

in which t_e = equivalent hydration period (maturity), defined in the sequel. Values $a_1 = 10^{-13}$ m/s, $a_2 = 40$ days agree well with the test data of Powers, et al. (39) for a Type I cement paste of water-cement ratio 0.7 [see Fig. 3(*b*)]. For a mature paste, the values of a_0 range from 10^{-10} m/s to 10^{-14} m/s (6,35).

Alternatively, we can determine reference permeability a_0 from its previously mentioned relationship to capillary porosity, due to Powers (39). This relationship appears to hold at any age, and the decrease of capillary water content with the progress of hydration (or age) may be estimated according to Ref. 39 [see Fig. 3(*b*)]. Instead of determining the reference permeability directly, we may evaluate it also from the diffusivity, C_0, in reference conditions (see Ref. 6); $C_0 = a_0/g_w$ in which $g_w = 9{,}806$ N/m^3 = unit weight of liquid water, and β = bulk compressibility of concrete (6).

Eq. 13 indicates permeability to be continuous when passing the saturation point, $p_s(T)$. However, for some concretes, such as lean dam concretes, permeability under hydraulic overpressure at low temperature may greatly increase when passing the saturation point (see Ref. 6).

Hydration and Dehydration of Water in Concrete

The amount of free water that is released upon heating into the pores of concrete due to dehydration has a great influence on pore pressures. It obviously depends on the amount of hydrated water before heating, which, in turn, is a function of the degree of hydration. The degree of hydration before heating depends on the age of concrete as well as its temperature and humidity history. It is also important whether the initial heating to high temperature occurs slowly or rapidly; if temperature is raised up to 100° C slowly, substantial amounts of water can become hydrated in the process and would then be available for dehydration at high temperatures.

The degree of hydration may conveniently be referred to the equivalent hydration period (maturity), t_e, which represents the period of hydration at 25° C in water, needed to give the same degree of hydration as the actual time period gives at variable h and T. It is defined, for $0 < T < 100^\circ$ C, as (7,9) $t_e = \int \beta_T \beta_h\, dt$, in which

$$\beta_h = [1+(3.5-3.5h)^4]^{-1};\quad \beta_T = \exp\left[\frac{U_h}{R}\left(\frac{1}{\hat{T}_0}-\frac{1}{\hat{T}}\right)\right] \qquad (17)$$

where t = actual time; $U_h/R = 2700^\circ$ K; and U_h = activation energy of hydration. By fitting the test results of Powers and Brownyard at 25° C (39), it has been found that [Fig. 1(*c*)]

$$w_h(t_e) \approx 0.21c\left(\frac{t_e}{\tau_e+t_e}\right)^{1/3};\quad \tau_e = 23 \text{ days} \qquad (18)$$

Dehydration of the hydrate water begins at about 120° C, and the amount of water that is dehydrated when reaching various temperatures is experimentally obtained by weight loss measurements on heated specimens. The amount of dehydrated water, w_d (per m^3 of concrete), can be expressed as

$$w_d = w_h^{105} f_d(T) \qquad (19)$$

in which w_h^{105} = the hydrate water content at 105° C. Typical values of $f_d(T)$ are plotted in Ref. 28. The values of $f_d(T)$ have been determined in a computer program by interpolation from a set of values.

Heat Conductivity and Heat Capacity of Concrete

Although heat conductivity b_0 slightly increases with water content and mildly varies with temperature as a result of changes in pore structure, the variations are small. Therefore, b_0 has been considered to be constant in all computations. Typical values of b_0 (for standard weight concretes) range from 0.18 cal/cm · s · ° C–0.36 cal/cm · s · ° C (27).

The heat capacity of concrete, C, consists of the heat capacity, $\rho_s C_s$, corresponding to the mass, ρ_s, of solid microstructure without any hydrate water (per m^3 of concrete), minus the heat loss (per m^3 of concrete) that is due to heat of dehydration, C_d (per kg of w_d). Therefore

$$\rho C\frac{\partial T}{\partial t} = \rho_s C_s \frac{\partial T}{\partial t} - C_d\frac{\partial w_d}{\partial t} \qquad (20)$$

The heat of sorption, C_a (Eq. 6), may be expressed as a sum of the latent heat of water [representing mainly the heat of vaporization of liquid water; Fig. 1(*b*)] and the heat of water adsorption, C_{ad}, on pore walls, i.e.

$$C_a\frac{\partial w}{\partial t} = \frac{\partial[w_c H(p,T)]}{\partial t} - C_{ad}\frac{\partial w_{ad}}{\partial t} \qquad (21)$$

in which H represents the enthalpy of liquid water as a function of p and T, given in the steam tables (3); w_c = amount of capillary water (per m^3 of concrete); w_a = amount of adsorbed water (per m^3); and $w = w_c + w_{ad}$ (plus the mass of vapor, which is negligible). Further complication arises from changes of heat capacity of solids in concrete, which reflect various changes in the microstructure of cement gel as well as the crystal structure of aggregate. In view of all these complexities, and because variations in C are not too large, it has been decided to refrain in computations from taking into account individual components of C (Eq. 20). Instead, an empirical temperature dependence of C has been used in computations (27,28), irrespective of w. Also C_a has been neglected because it contributes much less than C.

The heat of vaporization [Fig. 1(*b*)] with dehydration has recently been considered by Cheung and Baker (18). To be able to obtain analytical solutions, they assumed the heat diffusion problem to be linear and the release of the latent heat of vaporization to occur suddenly, upon passing 100° C, regardless

of the variation of w. Although this is a simplification (because the latent heat evolves by dehydration and vaporization through a wide range of temperatures), their study indicated that in concrete the effect of heats of dehydration and vaporization is rather small. The present finite element studies led to the same conclusion. This is largely due to the fact that water constitutes a small portion of the mass of concrete.

Moisture and Heat Transmission at Surface

In the first approximation, the moisture flux from the surface of concrete to the environment may be considered to be linearly dependent on the difference of the pore pressure, p_b, just under the surface of concrete and the water vapor pressure, p_{en}, in the environment:

$$\underline{n} \cdot \underline{J} = B_w(p_b - p_{en}) \text{ (at surface)} \quad \ldots \quad (22)$$

in which B_w = surface emissivity of water; and $\underline{n}$ = unit outward normal at the surface. A perfectly sealed surface of concrete ($\underline{J} = 0$) is a limiting case for $B_w = 0$, and perfect moisture transmission at the surface ($p_b = p_{en}$) is a limiting case for $B_w \to \infty$.

The heat flux, q, across the surface of concrete is, in the first approximation, linearly dependent upon the difference of surface temperature T_b and environmental temperature T_{en} (16). Adding the rate of heat loss due to the latent heat of moisture vaporization, we have

$$\underline{n} \cdot \underline{q} = B_T(T_b - T_{en}) + C_w \underline{n} \cdot \underline{J} \text{ (at surface)} \quad \ldots \quad (23)$$

in which B_T = surface emissivity of heat; and C_w = isobaric heat of vaporization of water from liquid state [Fig. 1(*b*)]. A perfect thermal insulation of the surface ($q = 0$) is obtained for $B_T = 0$, and a perfect heat transmission at the surface ($T_b = T_{en}$) is obtained for $B_T \to \infty$. More accurately, especially at high temperatures, the heat flux across the surface depends on fourth powers of absolute temperatures (16), but for the sake of simplicity this has not been used in computations. Fits of the weight loss experiments were satisfactory for $B_T = 0.0001$ cal/min·cm^2·° C and $B_w \to \infty$.

Finite Element Computation of Moisture and Heat Transfer in Concrete

For the sake of simplicity, only the one-dimensional problem for transfer in the radial direction, r, of polar coordinates will be considered. Noting that $\partial w/\partial t = (\partial w/\partial p)(\partial p/\partial t) + (\partial w/\partial T)(\partial T/\partial t)$, and eliminating fluxes $\underline{J}$ and $\underline{q}$ from Eqs. 2, 4, 5, and 6, we may reduce the field equations for moisture and heat transfer to the form

$$\frac{\partial}{\partial r}\left(a\frac{\partial p}{\partial r}\right) + \frac{\partial}{\partial r}\left(a_1\frac{\partial T}{\partial r}\right) + \frac{a}{r}\frac{\partial p}{\partial r} + \frac{a_1}{r}\frac{\partial T}{\partial r} + A_1\frac{\partial p}{\partial t} + A_2\frac{\partial T}{\partial t} + A_3 = 0 \quad (24)$$

$$\frac{\partial}{\partial r}\left(\frac{\partial T}{\partial r}\right) + \frac{b}{r}\frac{\partial T}{\partial r} + A_4\frac{\partial T}{\partial r} + A_5\frac{\partial T}{\partial t} + A_6\frac{\partial p}{\partial t} + A_7 = 0 \quad \ldots \quad (25)$$

$$\text{in which} \quad A_1 = -\frac{\partial w}{\partial p}; \quad A_2 = -\frac{\partial w}{\partial T}; \quad A_3 = \frac{\partial w_d}{\partial t} \quad \ldots \quad (26)$$

$$A_4 = -aC_w\frac{\partial p}{\partial r} - a_1C_w\frac{\partial T}{\partial r}; \quad A_5 = C_a\frac{\partial w}{\partial T} - \rho C;$$

$$A_6 = C_a\frac{\partial w}{\partial p}; \quad \text{and} \quad A_7 = 0 \quad \ldots \quad (27)$$

Similarly, Eqs. 2 and 4 for $\underline{J}$ and $\underline{q}$ may be substituted in Eqs. 22 and 23 to yield the boundary conditions in terms of only p and T:

$$a\frac{\partial p}{\partial r} + a_1\frac{\partial T}{\partial r} + B_w(p_b - p_{en}) = 0 \quad \ldots \quad (28)$$

$$b\frac{\partial T}{\partial r} - C_w a\frac{\partial p}{\partial r} - C_w a_1\frac{\partial T}{\partial r} + B_T(T_b - T_{en}) = 0 \quad \ldots \quad (29)$$

Eqs. 24 and 25 along with the boundary conditions in Eqs. 22 and 23 at $r = r_1$ and $r = r_2$ may be equivalently expressed by means of the variational equations

$$\int_{r_1}^{r_2} \text{LHS (Eq. 24)}\,\delta p\,dr - [\text{LHS (Eq. 28)}\,\delta p]_{r_1}^{r_2} = 0 \quad \ldots \quad (30)$$

$$\int_{r_1}^{r_2} \text{LHS (Eq. 25)}\,\delta T\,dr - [\text{LHS (Eq. 29)}\,\delta T]_{r_1}^{r_2} = 0 \quad \ldots \quad (31)$$

which must hold for any admissible variations δp and δT. LHS denotes the left-hand side of the equation.

To formulate a finite element scheme, we may apply a Galerkin-type procedure (30,45). We integrate by parts so as to get rid of the second spatial derivatives of p and T and at the same time eliminate derivatives from the boundary terms in Eqs. 30 and 31. Introducing finite elements in the radial direction, and choosing the interpolation (shape) functions N_i (of ith element) to be linear (triangular), we have $p = \Sigma\, p_i(t)\, N_i(r)$ and $T = \Sigma\, T_i(t)\, N_i(r)$, with $i = 1, 2$. Imposing the condition that the variational equation must hold for any admissible variations $\delta p_i(r)$ and $\delta T_i(r)$, we obtain:

$$\mathbf{K}_1\dot{\mathbf{p}} + \mathbf{K}_2\dot{\mathbf{T}} + \mathbf{K}_3\mathbf{p} + \mathbf{K}_4\mathbf{T} + \mathbf{F}_1 = 0; \quad \mathbf{K}_5\dot{\mathbf{T}} + \mathbf{K}_6\dot{\mathbf{p}} + \mathbf{K}_7\mathbf{T} + \mathbf{F}_2 = 0 \quad \ldots \quad (32)$$

in which $\mathbf{p}$ and $\mathbf{T}$ are the column matrices of nodal values p_k and T_k of the whole structure; $\mathbf{F}_1$ and $\mathbf{F}_2$ are also column matrices; and $\mathbf{K}_1, \mathbf{K}_2, \ldots, \mathbf{K}_7$ are square matrices. Their components for individual elements (el) are:

$$K_{1_{ij}}^{el} = A_1\int_{el} N_iN_j dr; \quad K_{2_{ij}}^{el} = A_2\int_{el} N_iN_j dr;$$

$$K_{3_{ij}}^{el} = -a\int_{el}\frac{\partial N_i}{\partial r}\frac{\partial N_j}{\partial r}dr + a\int_{el}\frac{1}{r}\frac{\partial N_i}{\partial r}N_j dr - [B_w]_{surf};$$

$$K_{4_{ij}}^{el} = -a_1\int_{el}\frac{\partial N_i}{\partial r}\frac{N_i}{r}dr - a_1\int_{el}\frac{1}{r}\frac{\partial N_i}{\partial r}N_i dr;$$

$$F^{el}_{1_i} = A_3 \int_{el} N_i dr + [B_w p_{en}]_{surf};$$

$$K^{el}_{5_{ij}} = A_5 \int_{el} N_i N_j dr; \quad K^{el}_{6_{ij}} = \int_{el} N_i N_j dr;$$

$$K^{el}_{7_{ij}} = \int_{el} \left[A_4 \frac{\partial N_i}{\partial r} N_j - b \frac{\partial N_i}{\partial r} \frac{\partial N_j}{\partial r} + \frac{b}{r} \frac{\partial N_i}{\partial r} N_j \right] dr - (B_T)_{surf};$$

$$F_{2_i} = A_7 \int_{el} N_i dr + \left[B_T T_{en} + C_w a \frac{\partial p}{\partial r} + C_w a_1 \frac{\partial T}{\partial r} \right]_{surf} \quad \ldots\ldots\ldots (33)$$

in which the terms with subscript surf are nonzero only in case of a surface node.

The structural matrices, which are assembled by superposition of the element components in the usual way (45), are, in general, nonsymmetric. This is an unpleasant but inevitable feature; it originates from the lack of symmetry of field equations themselves (Eqs. 24 and 25), stemming from the fact that the effects of grad T on $\underline{J}$ and of grad p on $\underline{q}$ are not the same (Eqs. 1–4). Expressing $\underline{J}$ and $\underline{q}$ in terms of the gradients of proper thermodynamic driving forces (21,32,43), one should be able to achieve symmetry, based on Onsager reciprocity relations; but at the expense of an increased number of material parameters. The matrix differential equations in Eq. 32 may be integrated in time by a step-by-step procedure, applying a Crank-Nicholson-type implicit algorithm for diffusion equation (40). To this end we introduce discrete time steps $\Delta t = t_{n+1} - t_n$ ($n = 1, 2, \ldots$), and, replacing the time derivatives in Eq. 32 by central difference approximations, we obtain the following quasilinear algebraic equations for column matrices $\mathbf{p}$ and $\mathbf{T}$ at time t_{n+1}:

$$\left(\mathbf{K}_1 + \mathbf{K}_3 \frac{\Delta t}{2}\right) \mathbf{p}_{n+1} + \left(\mathbf{K}_2 + \mathbf{K}_4 \frac{\Delta t}{2}\right) \mathbf{T}_{n+1} = \left(\mathbf{K}_1 - \mathbf{K}_3 \frac{\Delta t}{2}\right) \mathbf{p}_n$$

$$+ \left(\mathbf{K}_2 - \mathbf{K}_4 \frac{\Delta t}{2}\right) \mathbf{T}_n - \mathbf{F}_1 \Delta t; \qquad \left(\mathbf{K}_5 + \mathbf{K}_7 \frac{\Delta t}{2}\right) \mathbf{T}_{n+1} + \mathbf{K}_6 \mathbf{p}_{n+1}$$

$$= \left(\mathbf{K}_5 - \mathbf{K}_7 \frac{\Delta t}{2}\right) \mathbf{T}_n + \mathbf{K}_6 \mathbf{p}_n - \mathbf{F}_2 \Delta t \quad \ldots\ldots\ldots\ldots\ldots\ldots (34)$$

The nonlinearity of the problem is hidden in the dependence of coefficients $\mathbf{K}_1, \ldots, \mathbf{K}_7, \mathbf{F}_1, \mathbf{F}_2$ upon unknowns $\mathbf{p}_{n+1}$ and $\mathbf{T}_{n+1}$. All coefficients ought to be evaluated for $\mathbf{p} = (\mathbf{p}_n + \mathbf{p}_{n+1})/2$ and $\mathbf{T} = (\mathbf{T}_n + \mathbf{T}_{n+1})/2$, and therefore iteration at each time step is requisite.

The foregoing axisymmetric solution has been programmed for a CDC computer. By setting r_1 to be very large, $r_1 >> r_2 - r_1$, the same program could also be applied to solve one-dimensional nonaxisymmetric problems.

Data Fitting and Identification of Material Parameters

The computer program just described has been used to fit experimental data that are available in the literature on the subject as well as some drying tests

conducted at Northwestern University for this purpose. The following test data were used: (1) Tests of England and Ross (23) up to 130° C, in which pore pressure and temperature distributions were measured in a concrete cylinder

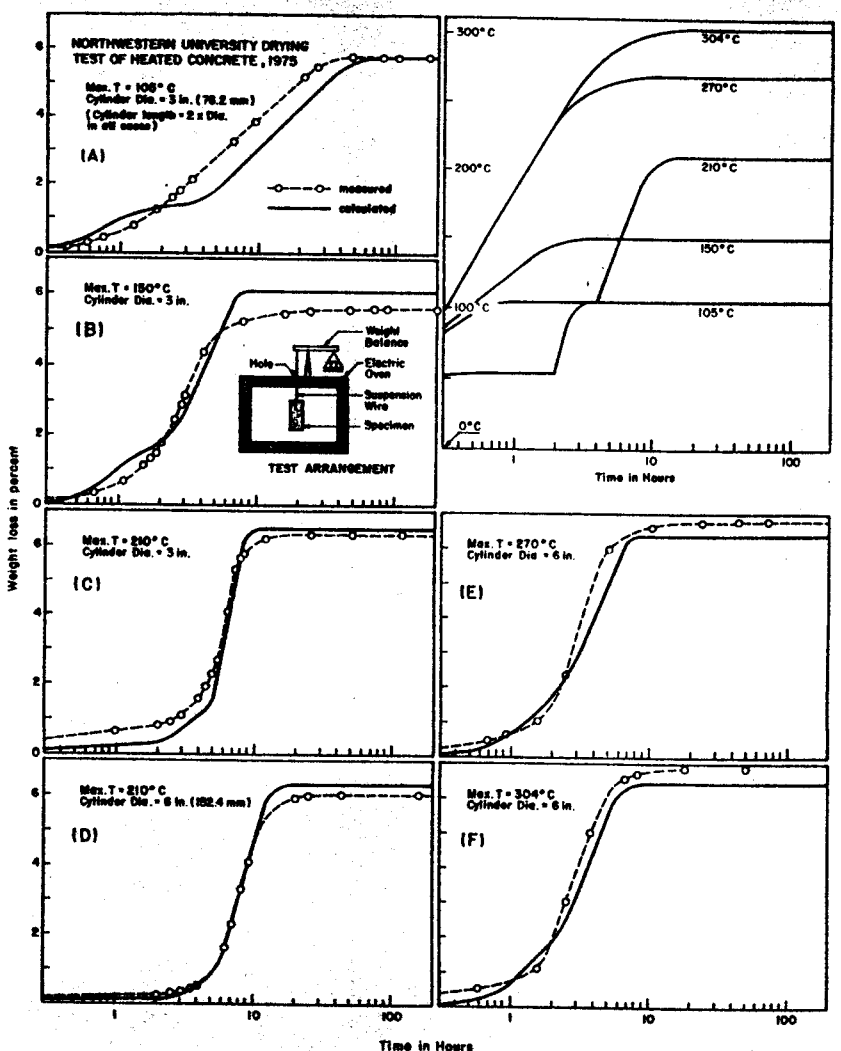

FIG. 4.—Fits of Weight Loss Tests at Northwestern University

that was sealed in a metallic jacket, heated at one end and vented at the other end, and thermally insulated along the cylindrical part of the surface; (2) tests of Zhukov and Shevchenko (46,47) up to 400° C, in which temperature and pore pressure distributions at various times were measured in large concrete

blocks (parallelepipeds), both exposed and jacketed, heated from one side and losing moisture (if exposed) to all sides; and (3) tests conducted by the writers at Northwestern University (up to 300° C), in which the rate of weight loss of concrete cylinders of various sizes, unsealed and exposed in an oven to temperatures from 105° C to 300° C, was measured. For detailed information on test data see Appendix I.

The material parameters and the empirical functions were varied so as to identify those that fit best. The fits achieved are shown in Figs. 4 to 6. The test data, as well as the present theory, indicate that pore pressures in heated concrete generally do not exceed 10 atm and are orders of magnitude less than those that could be expected on heating water in a closed rigid container.

To determine the permeability dependence on temperature, the weight loss tests (Fig. 4) were essential. The dependence obtained was then adjusted so

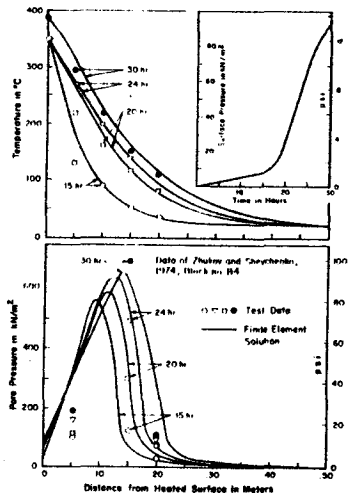

FIG. 5.—Fits of Temperature and Pore Pressure Distributions Measured by Zhukov and Shevchenko (46,47)

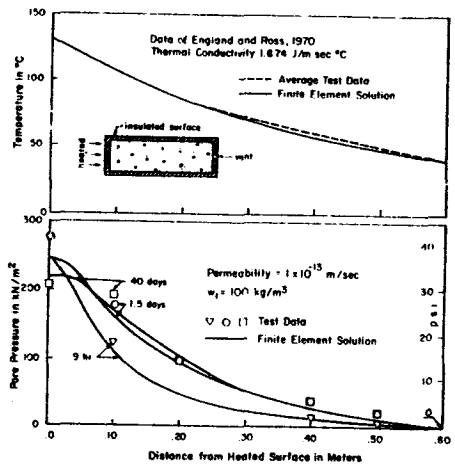

FIG. 6.—Fits of Temperature and Pore Pressure Distributions Measured by England and Ross (23)

as to fit also the tests of Zhukov and Shevchenko (46,47) as well as England and Ross (23). These tests, however, primarily provided information about the pore pressure dependence on w and T and about the change of porosity due to pressure. Function $f_1(h)$, previously determined in Eq. 13, was needed to delay the decrease of pore pressure in the drying region near the heated surface of Zhukov and Shevchenko's blocks and to fit the weight loss tests. This function also influenced the location of the peak value of pore pressure. The shape of the isotherm (w-p relationship) in nonsaturated region strongly influenced pore pressures and the rate of drying of concrete. In the saturation region, the pore pressure was controlled primarily by the variation of porosity, n (Eq. 10); if porosity grows too slowly while the temperature rises, then the pore pressure becomes too large. The width of the saturation transition region ($0.96 < p/p_s < 1.04$) also affected the pore pressure; if this range is too wide, it

would slow down the movement of water out of the saturated region, which would result in excessive buildup of pore pressure. Estimation of the saturation water content w_1 at 25° C, which is a linear function of porosity n, also influences pore pressure because if w_1 is small, then porosity is also small, which gives a low estimate of permeability and thus results in an increase of pore pressure if concrete is heated. The value of w_1 was estimated for the test data in Figs. 5 and 6 according to Powers and Brownyard's theory (39). Neville (35) gives a slightly different expression.

Various numerical difficulties had to be overcome. For example, the derivatives, $\partial w/\partial p$ and $\partial w/\partial T$, were initially evaluated from tangent slopes of the p-w-T relation at midsteps, $t_n + \Delta t/2$. However, in time steps when the boundaries of the saturation transition range (0.96 and 1.04) were crossed, great errors resulted because of a sharp change in slope of w versus p within the increment Δp. This has been remedied by evaluating the derivative from the increments of p and T for the whole time step, which causes the end point to stay exactly on the isotherm. Another numerical difficulty, consisting of spurious oscillations of the solution, occurred at the boundary when perfect heat transfer was assumed and a sudden change of temperature at the surface was considered. This was resolved by inserting very thin finite elements at the exposed surface.

It must be also pointed out that some error in data analysis is due to using a one-dimensional computer program in order to save computation costs. The specimens definitely were not in a one-dimensional state. Nevertheless, this error is undoubtedly less serious than the uncertainties and simplifications in material description. To minimize this error, the fitting of the weight loss of cylinders (of diameter D) that were not sealed at ends (Fig. 4) was done under the assumption that the rate of drying was, on the average, the same as for a cylinder of some equivalent diameter, D_1, that is sealed at ends. Diameter D_1 was determined from the condition $k_s(V/S) = k_{s_1}(V_1/S_1)$ in which V/S and V_1/S_1 are the ratios of exposed surface to volume for specimens of diameters D and D_1; k_s and k_{s_1} are the correcting shape factors for shrinkage and drying from Ref. 10; $k_{s_1} = 1.15$; and k_s was estimated as 1.4 in relation to the value 1.55 that applies for a cube (10). For test cylinders with diameters of 7.5 cm and 15 cm and lengths of 15 cm and 30 cm, respectively, this provided $D_1 = 7.02$ cm and 14.22 cm. This was then used in computations for Fig. 4.

Some data, unfortunately, were not reported with all relevant details. In case of Zhukov and Shevchenko's test (46,47) the values of surface temperatures were not given; therefore, the temperature values measured immediately below the surface were used as a prescribed input. In one of these tests, the heated specimen was in a metallic jacket, but the pore pressure neither at the surface nor between the jacket and the surface was reported. Fortunately, from the pore pressure-time curve given, it was possible to extrapolate the pore pressure values to the surface, as plotted in Fig. 5.

Conclusions

1. Although moisture transport is generally controlled by the gradients of both moisture concentration and temperature, it appears that for concrete it is possible to use the gradient of a single potential, i.e., the pore pressure. For nonsaturated concrete, pore pressure must be regarded as the pressure

in vapor rather than in capillary water. The gradient of pore pressure yields not only the moisture flux due to the concentration gradient (Fick's law) but also the flux due to the temperature gradient (Soret flux).

2. The permeability dependence on temperature exhibits an upward jump by two orders of magnitude when temperature passes 100° C. Up to about 100° C, the temperature dependence of permeability appears to be determined by activation energy, which agrees with the hypothesis that the moisture is controlled by the transfer migration of water molecules along adsorbed water layers. Well above 105° C, permeability appears to change relatively little with temperature, which suggests that the moisture transfer might be governed by viscosity of steam or liquid water.

3. The physical explanation of the jump in permeability at 100° C must be consistent with the preceding conclusion and also with the facts that: (a) In dense cement pastes the capillaries are not continuous; (b) the flow at room temperature is controlled by migration of absorbed water molecules; and (c) porosity is only modestly increased by heating. A possible explanation is that the flow is governed by "necks" of negligible volume on the flow passages. At room temperature, these necks are assumed to be of subcapillary size, and the flow then consists of adsorbed water migration. As temperature exceeds 100° C, the necks become much wider, allowing rapid flow of steam and liquid water.

4. The pore volume available to free water (capillary porosity) must be assumed to increase in proportion to the amount of chemically combined water that is released by dehydration due to heating. Furthermore, above the saturation pressure, the pore space available to free water must be assumed to increase with increasing pressure. Without these two hypotheses the calculated pressures would be far higher than observed.

5. Thermodynamic "steam tables" may be used for calculation of pore pressures in saturated concrete, but only under the foregoing assumptions.

6. The temperature effect on the isothermal relationship of water content and pore pressure in nonsaturated concrete is, approximately, a power function. The water content for which the saturation point is reached decreases with increasing temperature. Transition of the isotherms from nonsaturated to saturated states appears to be gradual rather than sudden.

7. The present theory rests on rather limited test data, which essentially serve to calibrate equations whose form is obtained largely by physical reasoning. Further test data are particularly needed on pore space and permeability beyond 100° C.

Acknowledgments

Support by the National Science Foundation under Grants ENG75-14848 and ENG-14848-A01 is gratefully acknowledged. Thanks are also due to Air Force Office of Scientific Research for partial support of the final phase of the work under Grant AFOSR-74-2733.

Appendix I.—Additional Information on Test Data and Parameters Used

Fig. 3.—Specimens were moist cured for 3 days at 24° C and 43 days at 60° C, dried to test humidity at 90° C for 13 days, and stored at 24° C until tested. Weight ratio of cement: fine aggregate (up to 3/8 in.); coarse aggregate (3/8 in.–3/4 in.); water = 1:2.03:2.64:0.425. Portland cement: Type III, 172 kg/m^3, slump: 4 in.; limestone aggregate. Monfore gages were inserted in wells to the center of specimens (6-in. × 12-in. cylinders).

Fig. 4.—Specimens were moist cured for 7 days at 25° C and then kept moist at 4° C until tested. Weight ratio of cement: fine Elgin aggregate (No. 4 to 5/8 in.); coarse Elgin aggregate (3/8 in.–3/4 in.); Elgin sand: water = 1:2.33:2.33:3.68:0.74; Portland cement: Type I, 227 kg/m^3; slump: 3 in.; cylindrical strength: 4,000 psi–4,500 psi. The parameters for tests A to F in Fig. 4 are: Age at test, in days = 35, 44, 28, 59, 63, and 66. Initial weight (kg) = 1.59, 1.60, 1.59, 12.64, 12.91, and 12.82. Permeability (10^{-12} m/s) = 1.3, 1.2, 1.2, 1.2, 1.0, and 1.0. Estimated saturation water content (kg/m^3) = 140, 135, 135, 135, 135, and 135. Thermal conductivity = 100.0 J/m·s·° C in all cases.

Fig. 5.—Specimen Nos. B2, B3, B4, and B7 were moist cured for 7 days, then stored at 70%–75% relative humidity at 18° C until tested. Weight ratio of cement: very fine powder of fire brick: fire brick sand: fire brick aggregate: water = 1:1:1.42:2.33:1. Portland cement: 300 kg/m^3; unit weight of concrete: 2,080 kg/m^3; cube strength: 300 kgf/cm^2–400 kgf/cm^2; porosity: 12%–15%. Specimen no. B4 in Fig. 2 was in metallic jacket. Age of concrete: 50 days; relative pore humidity: 95%. Specimen size: 0.50 m × 1.45 m × 1.05 m except specimen No. B3 for which the thickness is 0.20 m. Estimated saturation water content at 25° C is 190 kg/m^3. Permeability = 8.3×10^{-12} m/s for all cases; but for specimen No. B4, it is 2.5×10^{-12}. Thermal conductivity = 20.9 J/m·s·° C. Maximum pore pressures (kN/m^2) measured in blocks B3 to B7 are 360, 320, 690, and 300. Calculated maximum pore pressure (kN/m^2) are 330, 380, 670, and 400.

Fig. 6.—Specimen was cured in a metallic jacket at 20° C until tested at age of 28 days. Weight ratio of portland cement Type I: fine aggregate (up to 3/16 in.): coarse aggregate (rounded flint gravel up to 3/8 in.): water = 1:2.67:4.0:0.6. Specific surface of cement 3,350 cm^2/g.

Appendix II.—References

1. Al-Alusi, H. R., Bertero, V. V., and Polivka, M., "Effects of Humidity on the Time-Dependent Behavior of Concrete under Sustained Loading," *Report No. UC SCSM 72-2*, Structural and Material Research, Department of Civil Engineering, University of California, Berkeley, Calif., Jan., 1972.
2. Argyris, J. H., Warnke, E. P., and Willam, K. J., "Computation of Thermal and Moisture Fields in Massive Concrete Structures via Finite Elements" (in German), *Deutscher Ausschussfür Stahlbeton*, Heft 278, W. Ernst & Sohn, West Berlin, Germany, 1977.
3. "ASME Steam Tables, 1967," *Thermodynamic and Transport Properties of Steam*, 2nd ed., American Society of Mechanical Engineering, 1967.
4. Bažant, Z. P., "Thermodynamics of Interacting Continua with Surfaces," *Nuclear Engineering and Design*, Vol. 20, 1972, pp. 477–505.
5. Bažant, Z. P., "Some Questions of Material Inelasticity and Failure in the Design of Concretes Structures for Nuclear Reactors," *Transactions*, 3rd International Conference on Structural Mechanics in Reactor Technology, London, England, Sept., 1975, compiled by J. A. Jaeger, published by Commission of European Communities, Brussels, Belgium, Vol. 3, Paper H1/1.

6. Bažant, Z. P., "Pore Pressure, Uplift, and Failure Analysis of Concrete Dams," *Preprints,* Symposium on "Criteria and Assumptions for Numerical Analysis of Dams," International Commission on Large Dams, Swansee, England, Sept., 1975.
7. Bažant, Z. P., "Theory of Creep and Shrinkage in Concrete Structures: A Précis of Recent Developments," *Mechanics Today,* Vol. 2, Pergamon Press, New York, N.Y., 1975, pp. 1–93.
8. Bažant, Z. P., "Review of Literature on High Temperature Behavior of Concrete," *Report ORNL-TM-514S,* Oak Ridge National Laboratory (Contract W-7405-eng. 26), Tenn., Jan., 1976, pp. 71–142.
9. Bažant, Z. P., and Najjar, L. J., "Nonlinear Water Diffusion in Nonsaturated Concrete," *Materials and Structures,* Paris, France, Vol. 5, 1972, pp. 3–20.
10. Bažant, Z. P., Osman, E., and Thonguthai, W., "Practical Formulation of Shrinkage and Creep of Concrete," *Materials and Structures,* Paris, France, Vol. 9, No. 54, 1977, pp. 395–404.
11. Becker, J. M., and Bresler, B., "A Computer Program for the Fire Response of Structures—Reinforced Concrete Frames," *Report UCB FRG 74-3,* Structural Engineering and Structural Mechanics Department of Civil Engineering, University of California, Berkeley, Calif., Aug., 1974.
12. Becker, J. M., and Bresler B., "Reinforced Concrete Frames in Fire Environments," *Journal of the Structural Division,* ASCE, Vol. 103, No. ST1, Proc. Paper 12688, Jan., 1977, pp. 211–224.
13. Bertero, V. V., Bresler, B., and Polivka, M., "Instrumentation and Techniques for Study of Concrete Properties at Elevated Temperatures," American Concrete Institute International Seminar on Concrete for Nuclear Reactors, West Berlin, Germany, Oct., 1970.
14. Bremer, F., "Multi-Layer (Double-Wall) Prestressed Concrete Pressure Vessel," *Nuclear Engineering and Design,* North-Holland Publishing Co., Amsterdam, Netherlands, No. 5, 1967, pp. 183–190.
15. Brunauer, S., *The Adsorption of Gases and Vapors,* Vol. 1, Princeton University Press, Princeton, N.J., 1943.
16. Carslaw, H. S., and Jaeger, J. C., *Conduction of Heat in Solids,* 2nd ed., Oxford University Press, Oxford, England, 1973.
17. Cary, J. W., *Proceedings,* Soil Science Society of America, Vol. 30, 1966, pp. 428–433.
18. Cheung, F. B., and Baker, J., "Transient Dehydration Model for Concrete," *Technical Report,* Reactor Analysis and Safety Division, Argonne National Laboratory, Argonne; Ill., 1976.
19. Copeland, L. E., and Bragg, R. H., "Self-Desiccation in Portland Cement Pastes," *Proceedings,* American Society for Testing Materials, No. 204, Feb., 1955 (also Portland Cement Association, *Bulletin 52*).
20. Copeland, L. E., and Hayes, J. C., "Determination of Nonevaporable Water in Hardened Portland Cement Paste," American Society of Testing Materials, Bulletin No. 194, Dec., 1953, pp. 70–74.
21. DeGroot, S. R., and Mazur, P., "Nonequilibrium Thermodynamics," North Holland-Interscience Publications, New York, N.Y., 1962.
22. Dougill, J. W., "Conditions for Instability in Restrained Concrete Panels Exposed to Fire," *Magazine of Concrete Research,* Vol. 24, 1972, pp. 139–148.
23. England, G. L., and Ross, A. D., "Shrinkage, Moisture, and Pore Pressures in Heated Concrete," *Proceedings,* American Concrete Institute International Seminar on Concrete for Nuclear Reactors, Special Publication No. 34, West Berlin, Germany, Oct., 1970, pp. 883–907.
24. England, G. L., and Sharp, T. J., "Migration of Moisture and Pore Pressure in Heated Concrete," *Proceedings,* First International Conference on Structural Mechanics in Reactor Technology, Paper H2/4, Berlin, Germany, 1971.
25. Feldman, R. F., and Sereda, P. J., "A Model of Hydrated Portland Cement Paste as Induced from Sorption-Length Change and Mechanical Properties," *RILEM,* Paris, France, *Bulletin No. 6,* 1968, pp. 509–519.
26. Fischer, R. "On the Behavior of Cement Mortar and Concrete at High Temperatures" (in German), *Deutscher Ausschuss fur Stahlbeton,* Heft 216, W. Ernst and Sohn, West Berlin, Germany, 1970.
27. Harmathy, T. Z., "Thermal Properties of Concrete at Elevated Temperatures," *Journal of Materials,* American Society of Testing and Materials, Vol. 5, 1970, pp. 47–74.
28. Harmathy, T. Z., and Allen, L. W., "Thermal Properties of Selected Masonry Unit Concretes," *Journal of the American Institute,* Vol. 70, 1973, pp. 132–144.
29. Hundt, J., "Zur Wärme-und Feuchtigkeitsleitung in Beton, *Deutscher Ausschuss für Stahlbeton,* Heft 280, W. Ernst u. Sohn, West Berlin, Germany, 1977.
30. Hutton, S. G., and Anderson, D. L., "Finite Element Method: Galerkin Approach," *Journal of the Engineering Mechanics Division,* ASCE, Vol. 97, No. EM5, Proc. Paper 8448, Oct., 1971, pp. 1503–1519.
31. Jensen, B. M., "The Effect of Temperature on the Thermal Dilation of Concrete Conditioned to a Given Humidity," Graduate Student Research Report, Structural and Structural Mechanics Department, University of California, Berkeley, Calif., 1969.
32. Lykov, A. V., and Mikhailov, Y. A., *Theory of Energy and Mass Transfer,* Prentice Hall, Inc., Englewood Cliffs, N.J., 1961 (translated from Russian).
33. McDonald, J. E., "Moisture Migration in Concrete," *Technical Report C-75-1,* Concrete Laboratory, U.S. Army Engineers Waterways Experimental Station, Vicksburg, Miss., May, 1975.
34. *Mechanical Engineering,* American Society of Mechanical Engineers, Apr., 1977, p. 68.
35. Neville, A. M., *Properties of Concretes,* A Halsted Press Book, John Wiley and Sons, New York, N.Y., 1973.
36. Pihlajavaara, S. E., "On Practical Estimation of Moisture Content of Drying Concrete Structures," Concrete Laboratory—Technical Research Center of Finland, Otaniemi, Finland, 1974.
37. Pihlajavaara, S. E., and Väisänen, M., "Numerical Solution of Diffusion Equation with Diffusivity Concentration Dependent," The State Institute of Technical Research, Helsinki, Finland, 1965.
38. Pihlajavaara, S. E., and Tivsanen, K., "A Preliminary Study on Thermal Moisture Transfer in Concrete," Laboratory of Concrete Technology, No. 15, Otaniemi, Finland, 1970.
39. Powers, T. C., and Brownyard, T. L., "Studies of the Physical Properties of Hardened Portland Cement Pastes," Research Laboratory of the Portland Cement Association, *Bulletin 22,* Mar., 1948 (also ACI Journal, Vol. 43, Oct. 1946–Apr. 1967).
40. Rosenberg, D. U., *Methods for the Numerical Solution of Partial Differential Equations,* American Elsevier Publishing Co., Inc., New York, N.Y., 1969.
41. Schneider, U., "Physical Properties of Concrete Under Non-Steady State Conditions," *Proceedings,* 7th Congress, Fedération Internationale de la Précontrainte, New York, N.Y., 1974.
42. Weiss, R., and Schneider, U., "N_2-Sorptionsmessungen zur Bestimmung der Spezifischen Oberfläche und der Porenverteilung von Erhitztem Normalbeton," *Report,* Technische Universität Braunschweig, 1976.
43. Welty, J. R., Wicks, C. E., and Wilson, R. E., *Fundamentals of Heat and Mass Transfer,* John Wiley and Sons, New York, N.Y., 1969.
44. Winslow, D. N., and Diamond, S., "Specific Surface of Hardened Portland Cement Paste as Determined by Small-Angle X-Ray Scattering," *Journal of American Ceramic Society,* Vol. 57, 1974, pp. 193–197.
45. Zienkiewicz, O. C., *The Finite Element Method in Engineering Science,* McGraw-Hill Book Co. Ltd., London, England, 1971.
46. Zhukov, V. V., et al., "Thermophysical Analysis of Structures of Heat-Resistant Concretes," (Teplofizicheskie Raschety Konstrukcii iz Zharostoikogo Betona na AVM i CVM), NIIZhB, Volgograd, 1971.
47. Zhukov, V. V., and Shevchenko, V. I., "Investigation of Causes of Possible Spalling and Failure of Heat-Resistant Concretes at Drying, First Heating and Cooling," *Zharostoikie Betony (Heat-Resistant Concrete),* K. D. Nebrasov, ed., Stroiizdat, Moscow, U.S.S.R., 1974, pp. 32–45.

14077 HIGH TEMPERATURE CONCRETE DRYING

KEY WORDS: **Concrete properties; Concrete structures;** Diffusion; Drying; Finite element method; Fire resistance; Heat conductivity; **Nuclear reactors; Pore pressure;** Porosity; Porous materials; **Thermal properties;** Thermodynamics; Water transfer

ABSTRACT: A mathematical model for water transfer in concrete above 100°C is developed. Drying tests of heated concrete are reported and material parameters of the model are identified from these tests as well as other test data available in the literature. It is found that water transfer is governed principally by the gradient of pore pressure, which represents the pressure in vapor if concrete is not saturated. Permeability is found to increase about 200 times as temperature passes 100°C, which could be explained by a loss of necks on migration passages. The pore volume available to free water increases as dehydration due to heating progresses and as the pore pressure is increased. The temperature effect on pressure-water content (sorption) relations is determined. Thermodynamic properties of water are used to calculate pore pressures. A finite element program for coupled water and heat transfer is developed and validated by fitting test data.

REFERENCE: Bazant, Zdenek P., and Thonguthai, Werapol, "Pore Pressure and Drying of Concrete at High Temperature," *Journal of the Engineering Mechanics Division,* ASCE, Vol. 104, No. EM5, **Proc. Paper 14077,** October, 1978, pp. 1059-1079